

Electron density monitoring for the lower ionosphere using Schumann resonance analysis of magnetotelluric data

Debopriya Das¹, Sudha Agrahari¹, Arseny Shlykov² and Alexander Saraev²

¹Indian Institute of Technology Kharagpur, debopriyad128@gmail.com

²Saint Petersburg State University

SUMMARY

Utilizing Magnetotelluric (MT) data enables the estimation of electron density within the lower ionosphere layer. This estimation provides insight into the prevailing conditions of the lower ionosphere, thereby highlighting deviations from typical trends. These deviations manifest on a daily basis within the lower ionosphere, with notable shifts potentially indicating alterations in climatic conditions, whether anthropogenic or natural in origin. The paper explores Schumann resonance (SR) variation to analyze electron density fluctuations in India's Odisha region. Orthogonal magnetic and electric field data were collected from the Mahanadi Shear Zone of Odisha region, India, in the months of April and December 2017. A Fast Fourier transform is then performed on the data with a high frequency resolution of 0.015 Hz. Furthermore, spectral resolution in SR mode was achieved by averaging the power spectral magnitude of 64 data segments sampled at 64 Hz frequency with 4096 sample points. Notably, the study observed amplitude variations, particularly influenced by day-night transitions and sunset effects. Diurnal fluctuations in the first three SR modes of electromagnetic components were also observed, with maximum frequency variations noted at 0.38, 0.13, and 0.37 Hz for the initial three (first, second and third) Schumann resonance modes, respectively. Leveraging these insights, we have calculated ionospheric electron density at a particular hour for various stations in Odisha, offering valuable insights into sudden ionospheric disturbances.

These disturbances may be caused due to increase in greenhouse gas or aerosol concentrations, stemming from phenomena such as volcanic eruptions, major weather patterns, or industrial emissions. The Release of radon gas from subsurface owing to fault movement prior to an earthquake, changes the aerosol concentration in lower ionosphere. Additionally, occurrence of Schumann resonance can contribute to the study of short-term earthquake precursor, if the data is collected before an earthquake from any potential zone.

Keywords: Schumann Resonance, Magnetotelluric, Ionosphere, Electron density, Fast Fourier Transform

INTRODUCTION

Schumann (1952) proposed an Extremely low frequency (ELF) resonance in the earth-ionospheric waveguide, where lightning-generated electromagnetic waves travel the Earth's surface and return, showing a $2\pi n$ phase difference. Investigations by various researchers explored geomagnetic influences on SR modes (Hayakawa et al. (2005)). Studies revealed ionospheric conductivity affecting frequencies and also diurnal SR variations depend on observation points. Researchers highlighted the importance of SR variations in ionospheric characterization and disturbance monitoring. Ionospheric D-region's effective altitude dropped 3 km in 45 years; linked to higher greenhouse gases causing increased infrared cooling (Clilverd et al., 2017). Therefore, prolonged observation of reduced D-region electron

density values could be a valuable insight into climate change.

This analysis is based on magnetotelluric data acquired in Odisha, Mahanadi shear zone. Then time series analysis is applied with spectral enhancing and frequency resolution of 0.015Hz. Then hourly variation is observed along with day night and sunset effects. Then average variation of SR modes is seen, aiming to determine the distribution of ionospheric electron density at specific hours across different sites and of different days.

METHODOLOGY

When considering the earth-ionosphere boundaries to be perfectly conductive, various frequency modes can be obtained using the equation provided (Schumann, 1952),

EMIW2024 abstracts are distributed under the Creative Commons Attribution 4.0 Unported License. Authors retain the copyright of the abstract but grant any third party the right to use the abstract freely as long as its original authors and citation details are identified.

To view a copy of this license, visit <https://creativecommons.org/licenses/by/4.0/>

$$fn \equiv \frac{\omega_n}{2\pi} \approx \frac{c\sqrt{n(n+1)}}{2\pi R_E} = 10.6 \sqrt{\frac{n(n+1)}{2}} \text{ Hz}, \quad (1)$$

$n = \text{any integer}$, $c = \text{velocity of light}$, $R_E = \text{radius of the earth}$.

The initial five resonance frequencies are 10.6, 18.4, 26.0, 35.5, and 41.1 Hz. However, ionosphere does not exhibit perfect conductivity, leading to energy losses that decrease the resonance frequencies to 7.8, 14.1, 20.3, 26.3, and 32.5 Hz (Madden and Thomson, 1965).

Spectral Analysis of MT data

The time domain LF2 band data is segmented into N windows of 4096 seconds each (N=64 seconds) before undergoing individual Fourier transformations to convert them to the frequency domain. These segments are then combined, averaged to reduce noise, and visually represented in power spectra. As N increases, Schumann resonance modes become observable, stabilizing the spectrum and revealing the first three SR mode frequencies in the magnetic field component (Hx) power spectra. The aim was to determine the minimum N value needed to display SR mode frequencies clearly.

Estimation of Electron density in lower ionosphere

Schumann's initial (1952) work estimated lightning-induced electromagnetic resonance frequencies in the earth-ionosphere cavity using a basic vacuum model. Subsequent research by others emphasized the necessity of realistic dielectric permeability models for comprehending Schumann resonance (SR) frequencies. Roldugin *et al.* (1999) showed how electron density and base height impact SR frequencies, culminating in a quantitative model by Roldugin *et al.* (2003) that connects SR frequencies to ionospheric parameters through a two-layer model and a time-dependent exponential factor.

For the first non-conducting air layer

$$\varepsilon(z) = 1, \quad 0 \leq z < a \quad (2)$$

The second layer model for the D-region starting at $z=a$.

$$\varepsilon = \frac{\omega_{02}^2}{i\omega\vartheta_{e2}} \exp\left[\frac{z-a}{h}\right] = \frac{\sigma_2}{i\omega\varepsilon_0} \exp\left[\frac{z-a}{h}\right], \quad z > a. \quad (3)$$

Where, $\omega_{02} = \text{plasma frequency}$, $\vartheta_{e2} = \text{electron collision frequency}$, $h = \text{scale height}$. These parameters are given by Nickolaenko and Hayakawa, 2002; Bliokh *et al.*, 1980.

$$\omega_{02}^2 = \frac{N_2 e^2}{m_e \varepsilon_0}, \quad \sigma_2 = \frac{N_2 e^2}{m_e \vartheta_{e2}} = \frac{\omega_{02}^2 \varepsilon_0}{\vartheta_{e2}}, \quad (4)$$

Where, $N_2 = \text{electron density at } z=a$, $m_e = \text{mass of the electron}$.

Roldugin *et al.* (2003) derived the following formula using above consideration,

$$\omega = \frac{c\sqrt{n(n+1)}}{R_E} \cdot \frac{1}{\sqrt{1 + \frac{2h}{a} \left[\gamma - \ln\left(\frac{\omega_{02} h}{c} \sqrt{\frac{i\omega}{\vartheta_{e2}}}\right) \right]}}, \quad (5)$$

$n = \text{integers}$, and $\gamma = \text{Euler's constant}$ whose value is 0.577.

After linearizing the Equation 5, Roldugin *et al.* (2003) provided with the following form,

$$Re(f_2) = 13.7 + 0.56 \log_{10}(N_2/100) - 0.65(h - 4) + 0.086(a - 61), \quad (6)$$

$$Im(f_2) = -0.40 - 0.050 \log_{10}(N_2/100) - 0.045(h - 4) - 0.00094(a - 61), \quad (7)$$

$Re f_2 = \text{is the real part of second SR mode}$ and $Im f_2 = \text{imaginary part of second SR mode}$.

Following time series processing and filtering, the Schumann resonance modes obtained were utilized in conjunction with Equation 6 to calculate the electron density.

RESULTS

Magnetotelluric time series data first converted into frequency domain by Fast Fourier Transform and then filtered to reduce the noise and visibility of Schumann resonance frequency. Then those Schumann resonance frequencies are used to serve the final purpose of computing electron density value.

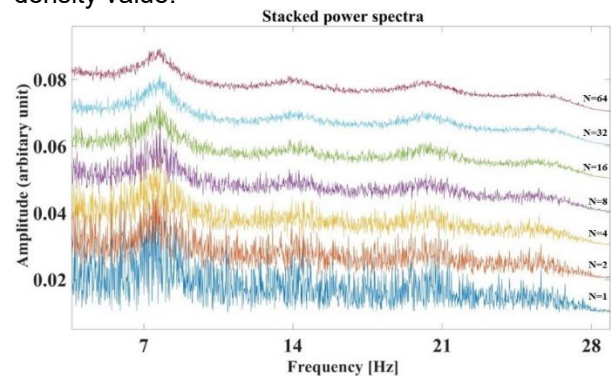


Figure 1. Stabilized stacked spectral density estimates for first three SR modes of magnetic field component Hx.

The inherent stabilization of the combined spectral approximations highlights the initial three Schumann Resonance (SR) modes specific to the magnetic field component Hx. The frequency is depicted on the horizontal axis, while the amplitude, presented in varied arbitrary scales, is shown on the vertical axis to illustrate different numbers of stacked segments (N). At N=64 desirable stabilization was achieved for our data set.

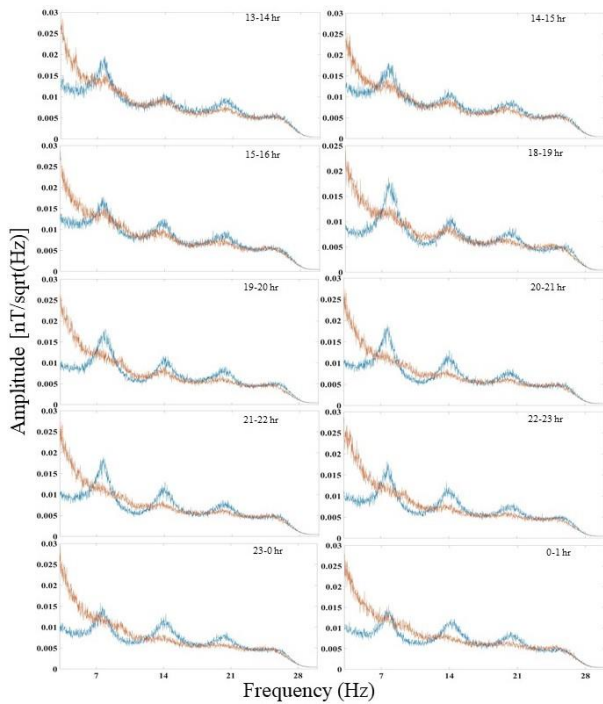


Figure 2. The changes in the amplitude-frequency spectrum of two magnetic field elements Hx and Hy (represented by blue and red color respectively) on an hourly basis.

Amplitude spectrum variation for Odisha, India site in Figure 2 shows two magnetic field components in LF2 band (64 Hz sampling). 4096 sample points meet Schumann resonance criteria with 0.015 Hz resolution for 0.03-32 Hz range, covering 10 h from 13:00 to 16:00 h and 18:00 to 01:00 h.

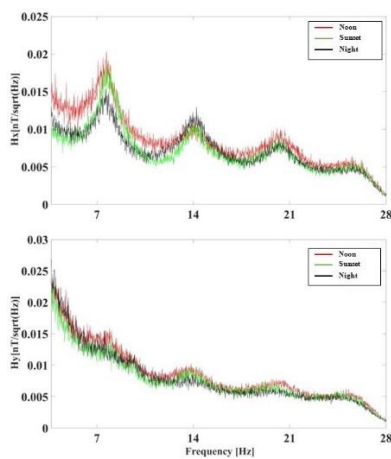


Figure 3. Noon, sunset and night time Amplitude spectral variation in Hx and Hy field components.

In Figure 3 the amplitude spectral variation of magnetic components (Hx and Hy) for the noon, night and sunset time is shown. From the figure it can be judged that during the noon time amplitude was little bit higher than the rest. 13:00-14:00 h was chosen as the noon time. The solar terminator (sunset) time taken from 18:00 h to 19:00 h and the night time was 23:00-00:00 h. One hour frequency spectrum analysis was done to see the amplitude spectral diurnal variation.

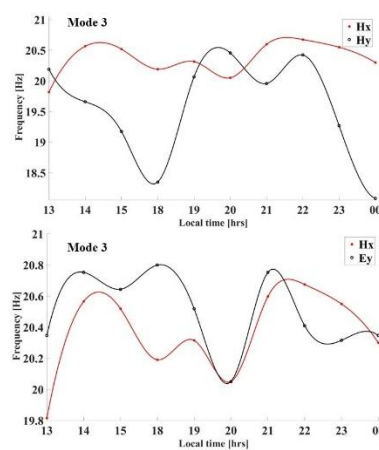


Figure 4. Diurnal fluctuations of frequency corresponding to the third Schumann resonance mode.

Figure 4 illustrates diurnal frequency changes of Schumann resonance mode 3. It shows magnetic components Hx and Hy with opposite polarization and electromagnetic components Hx and Ey with the same polarization. Within a single polarization, similar frequency shifts indicate similar information content, while opposite polarization components exhibit inverse frequency variations.

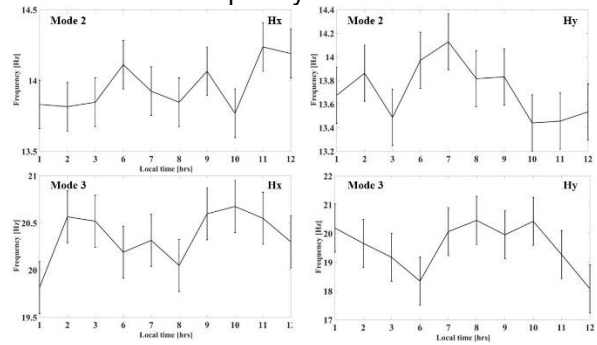


Figure 5. The average diurnal fluctuations of the second and third SR modes frequency of magnetic field component Hx and Hy.

In order to enhance statistical reliability, the average daily frequency fluctuations for second and third SR modes, along with their respective magnetic field components and standard deviations, are depicted in Figure 5. Typically, periodic frequency shifts are discernible across all field components. It's also worth noting that in certain components, the periodic pattern is not as readily discernible.

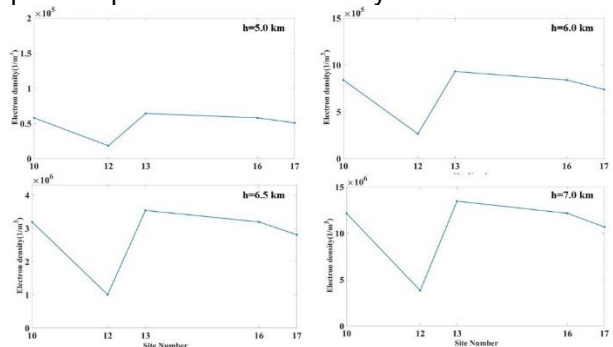


Figure 6. Using second SR mode frequency electron density is calculated for different scale height (h).

Equation 6 was used to calculate electron density variations from 18:00-19:00 for five distinct sites in Odisha across different days, plotted in Figure 6. Initial parameters included $a=55.00$ km, varied h values (5, 6, 6.5, and 7 km). Real frequencies from Schumann resonance modes were considered. Increasing scale height (h) exponentially boosts electrical conductivity, correlating with electron density from Equation 4, as shown in Figure 6.

DISCUSSION

According to Grimalsky *et al.* (2003), they studied the infiltration of electric and magnetic field components of Schumann resonances into the ionosphere, concluding that magnetic field component has 2-3 times higher penetration depth than electric field components. Based on that focusing mainly on magnetic field components, opposite phase variations between H_x and H_y components is observed at different times of the day along with similar phase variation in H_x and E_y , from Figure 5. For the first, second, and third Schumann resonance modes, frequency variations ranged from 1.65% to 3.04%, 1.3% to 1.9%, and 2.66% to 1.51%, respectively. Clilverd *et al.* (2017) established modal minima locations based on characteristics of the nighttime electron density profile in the D-region, offering advantages for long-term trend analysis due to reduced solar influence and increased sensitivity to potential anthropogenic changes. Referring to this an evening time was selected for the present study with different site and dates for the electron density monitoring.

CONCLUSIONS

The study involves examining the spectral characteristics of magnetotelluric data gathered from the Odisha region in India to investigate Schumann resonance frequency fluctuations and a study of electron density variation. Data from orthogonal horizontal electric and magnetic field components collected from different stations in the month of April and December 2017, serve as the foundation for this analysis. Employing the Fast Fourier Transform (FFT) algorithm, frequency spectra are generated with a precision of 0.015 Hz. While similar Schumann resonance frequency variations are seen from Figure 4 in components with identical polarization (H_x and E_y), and contrasting frequency variations are evident between the north-south (N-S) and east-west (E-W) magnetic field components (H_x and H_y respectively). The analysis uncovers a consistent cyclic change in Schumann resonance frequencies, although with varied phase alterations between the two magnetic field elements. Additionally, estimates of electron density fluctuations in the lower ionosphere are derived from observed Schumann resonance

frequencies for further studies related to climate change like lowering of ionospheric D-region and other disturbances in ionosphere. Also, the Schumann resonance frequency analysis can extend to the study of short time Earthquake precursor.

ACKNOWLEDGEMENT

The authors are thankful to Mr. Gaurav Kumar, Mr. Yashvant Singh, Mr. Amit Kumar and Dr. Akarsh Singh for their help in field work. Also, to Mr. Subhrajit Ghosh for the help in some mathematical understanding.

REFERENCES

- Schumann, W. O. (1952) U"ber die Strahlungslosen Eigenschwingungen einer leitenden Kugel die von Luftschicht und einer Ionosph"arenhu"lle umgeben ist, *Z. Naturforsch.*, 7a, 149– 154.
- R. Chand, M. Israil and J. Rai (2009) Schumann resonance frequency variations observed in magnetotelluric data recorded from Garhwal Himalayan region India. *Ann Geophys.*, 27, 3497-3507.
- M. Hayakawa, K. Ohta, A. P. Nikolaenko and Y. Ando (2005) Anomalous effect in Schumann resonance phenomena observed in Japan, possibly associated with Chi-chi earthquake in Taiwan. *Ann Geophys.*, 23(4), 1335-1346.
- M. A. Clilverd, R. Duthie, C. J. Rodger, R. L. Hardman and K. H. Yearby (2017) Long-term climate change in D-region. *Sci Rep* 7, 16683. <https://doi.org/10.1038/s41598-017-16891-4>.
- V. C. Roldugin, Y. P. Maltsev, A. N. Vasiljev, and E. V. Vashenyuk (1999) Changes of the first Schumann resonance frequency during relativistic solar proton precipitation in the 6 November 1997 event. *Ann. Geophys.*, 17, 1293– 1297.
- V. C. Roldugin, Y. P. Maltsev, A. N. Vasiljev, A. V. Shvets and A. P. Nikolaenko (2003) Changes Schumann resonance parameters during the Solar proton event of 14 July, 2000. *J. Geophys.* 109, A08304, doi: 10.1029/2002JA009495.
- V. Grimalsky, A. Kotsarenko, R. P. Enriquez and S. Koshevaya (2003) Penetration of electric and magnetic field components of Schumann resonances into the ionosphere. *IEEE International Symposium on Electromagnetic Compatibility, 2003. EMC '03.*, Istanbul, Turkey, 2003, pp. 753-755 Vol.2, doi: 10.1109/ICSMC2.2003.1429015.